Article

Assessment and Characterization of Duck Feathers as Potential Source of Biopolymers from an Upcycling Perspective

Sandra Alvarez [1,†], Nidal Del Valle Raydan [1,†], Isabelle Svahn [2], Etienne Gontier [2], Klaus Rischka [3], Bertrand Charrier [1] and Eduardo Robles [1,*]

[1] University of Pau and the Adour Region, E2S UPPA, CNRS, IPREM-UMR 5254, 40004 Mont de Marsan, France; sandra.alvarez@univ-pau.fr (S.A.); ndvraydan@univ-pau.fr (N.D.V.R.); bertrand.charrier@univ-pau.fr (B.C.)
[2] Bordeaux Imaging Center/Electronic Imaging, UAR 3420 CNRS US4 INSERM, 33000 Bordeaux, France; isabelle.svahn@u-bordeaux.fr (I.S.); etienne.gontier@u-bordeaux.fr (E.G.)
[3] Fraunhofer Institute for Manufacturing Technology and Advanced Materials (IFAM), 28359 Bremen, Germany; klaus.rischka@ifam.fraunhofer.de
* Correspondence: eduardo.robles@univ-pau.fr; Tel.: +33-558513770
† These authors contributed equally to this work.

Abstract: A comprehensive characterization of the physical and chemical properties of whole duck feathers from French mulard species, including their various categories and fractions (barbs, rachis, and calamus), was conducted to explore potential ways for utilizing this waste product. This analysis aimed to identify opportunities for valorizing these feathers and unlocking their untapped potential. Hence, the duck feathers were thoroughly characterized by a proximate analysis to determine their composition and theoretical heating value. Additionally, feathers underwent other analyses as Sodium Dodecyl Sulfate Polyacrylamide Gel Electrophoresis (SDS-PAGE) analysis, solvent behavior and chemical durability assessment, hydrophobicity testing, Fourier Transform Infrared (FT-IR) spectroscopy, Thermogravimetric Analysis (TGA), Differential Scanning Calorimetry (DSC), X-ray diffraction (XRD), and Scanning Electron Microscopy (SEM). The analyses revealed duck feather composition, molecular weight, stability in different environments, hydrophobicity, functional groups present, thermal behavior, crystallinity, and structural arrangement. Upon analysis, it was determined that duck feathers contain pure fiber keratin and possess characteristics that make them suitable for the production of high-value keratin-based products, including cosmetics, activated carbon for purification, materials for waterproofing, lightweight construction, and textile innovations, underscoring their potential to support sustainable and eco-friendly initiatives across various sectors.

Keywords: duck feathers; renewable resource; bio-based polymers; physical properties; chemical properties; high-value byproducts

1. Introduction

For several years, interest in using natural products from the agricultural sector has been increasing to cope with environmental issues such as the eventual depletion of fossil raw materials and the high use of non-renewable petroleum resources. In addition, the population growth on Earth affects agricultural production, which increases according to demand and can cause environmental damage. Every year, the poultry industry generates large quantities of by-products such as bones, skin, blood, fat, viscera, and feathers [1,2]. These by-products are generally unused and are dumped in landfills to be buried or incinerated [3]. Each of these two processes has disadvantages; burial can cause pollution of the soil, air, and water [4] around the location, and incineration, while destroying all infectious agents, releases polluting gases [4]. However, the reuse of these by-products has generated a growing interest for several years because they are inexpensive and renewable resources that could be reused in different industry sectors and can contribute economically

to provide additional funding for the poultry industry. Currently, feathers are commonly considered waste materials despite their limited utilization in producing feather meals, fertilizers, and biodiesel; the prevalent disposal methods for feather waste involve incineration or landfill burial, contributing to environmental damage and disease transmission.

On a local scale, the southwest of France, particularly the New Aquitaine region, is known to be the first place for producing fattened ducks in France [5]. Indeed, it alone represents 50% of the total French production. Furthermore, the palmipeds sector represents a major part of the food production in New Aquitaine. Fattened duck production is mainly dedicated to the public consumption of meat and *foie gras*. In 2015, French production amounted to 35.9 million fattened ducks, including 20.2 million grown in the New Aquitaine region, representing 56% of the total production in France [5]. The main species raised for meat and *foie gras* production in France is the mulard duck. It is a hybrid species resulting from the crossing of two duck species, between a male Muscovy duck (*Cairina moschata)* and a female Peking duck (*Anas platyrhynchos*) [6].

Ducks are slaughtered and then plucked for further processing of the meat. After plucking, feathers are dirty with a foul odor, including blood and other excrements containing microorganisms, bacteria, fungi, or other microbial toxins [7]. Feathers are separated to recover the down and small feathers, while the rest is stored in landfills where blood or other organic residues constitute a significant risk to human and animal health. Several recycling methods exist for all feathers to give a second life and create added-value products, from decoration to sports equipment or the medical sector [3]. The most common ways to recycle feathers consist of using them as fertilizer [8] due to their high content of nitrogen for plant growing operations, transforming feather meal in biodiesel with a green process by transesterification of the fat extracted [9] or using them as animal feed given its high protein content [10]. However, the desire and need to find alternatives to synthetic plastics has led to the emergence of another kind of feather valorization for the chemical sector. The feather composition is interesting because of its high keratin content: 91% keratin, 8% water, and 1% lipids [11]; therefore, feathers are a source of keratin. Keratin is known to be an insoluble cysteine-rich protein. Proteins are large and complex molecules essential to adequately functioning cells in body tissues and organs. They comprise a set of amino acids linked by peptide bonds, forming a polypeptide chain [11]. The stability of the keratin is made possible by the intramolecular and intermolecular disulfide bonds; thus, these proteins can exist in aggressive environments such as under high temperatures, in solvents, or in acidic and basic conditions [12]. The keratin secondary structure can be found in two stable configurations: α-helix and β-pleated sheet. These two configurations are found in animal species, but, more precisely, α-keratin is found in mammals, whereas β-keratin, named hard keratin, is found in reptilian and avian species [13]. α-helix configuration is a spiral/coiled coils arrangement, whereas β-pleated sheets are laterally packed parallel or antiparallel chains. Both configurations are stable thanks to hydrogen bonds between chains, hydrogen bonds inside the helix chain for α-helix configuration, and intermolecular hydrogen bonds for β-sheet pleated configuration [14,15].

Despite the growing popularity of feathers, there is a lack of scientific articles in the chemical sector that refer to duck feathers, the vast majority of publications being about chicken feathers. Indeed, the literature contains several reviews and papers on chicken feathers' physicochemical and mechanical properties [3,16,17]. In contrast, reviews of the complete characterization of duck feathers are almost non-existent, and it is crucial to characterize thoroughly a material before considering its valorization. Therefore, this work describes the complete characterization of duck feathers from the specific mulard species. Physicochemical properties are analyzed to better understand the similarities and differences between duck and chicken feathers to ensure that chicken feather recovery routes can be applied to duck feathers. In addition, it provides a better understanding of how this by-product can be upscaled to obtain chemical precursors and to elaborate materials.

2. Materials and Methods

2.1. Pre-Treatment of Feathers

White duck feathers of the mulard species were kindly provided by Plum'Export (Saint-Sever, France). The feathers received were collected without treatment or cleaning after plucking the ducks. Then, they were sorted manually and classified according to their size and morphology. They were classified into six different categories, represented in Figure 1. Each category was weighed to determine its mass percentage in a random mix based on 10 kg of sorted feathers. The categories range from the light down through small soft feathers to large stiff feathers. For this purpose, one hundred feathers of the three largest feather sizes were measured and weighed to know their average dimensional characteristics, represented in Table 1. The calamus, rachis, and barbs were manually cut. Much waste was also sorted, such as dry skin, feces, bones, dust, and slaughterhouse residues.
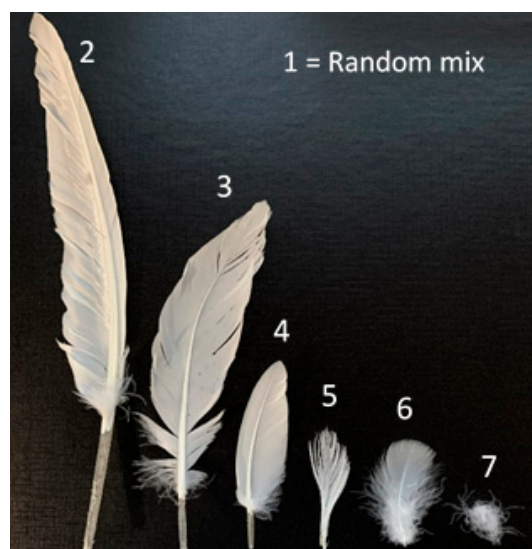

Figure 1. Different categories of duck feathers.

Table 1. Dimensional characteristics of each category.

Category	wt%	Whole-Feather Height (mm)	Whole-Feather Weight (g)	Calamus (wt%)	Rachis (wt%)	Barbs (wt%)
2	58.26	229.5	0.74	30	40	30
3	27.59	186.7	0.35	26	40	34
4	7.90	118.8	0.16	26	28	46
5	3.40	-	-	-	-	-
6	0.18	-	-	-	-	-
7	0.19	-	-	-	-	-
Waste	2.48	-	-	-	-	-

Feathers were cleaned after sorting. Cleaning is critical because poultry feathers often carry microorganisms and bacteria that are dangerous to humans. The most recurrent problem encountered is dried blood inside the calamus, especially of the large feathers. Therefore, roughly grinding the feathers with a 5 mm sieve was necessary to facilitate the cleaning. Then, the cleaning process consisted of three steps. The first cleaning was conducted with soap in hot water at 60 °C for 2 h, followed by filtration and rinsing under hot water to remove easily removable matter. Following this, a disinfection step with an ethanol/water mixture (60/40) at 60 °C for 30 min and filtration was conducted. Finally, the feathers were rinsed with hot water. After cleaning, the feathers are white and odorless,

air-dried at room temperature, and stored in closed containers. The feathers were ground to 200 μm using a Retsch ZM 200 mill for the following analyses.

2.2. Proximate Analysis

The physicochemical properties of the seven categories of the feathers and calamus, rachis, and barbs were analyzed to determine the percentages of moisture content, volatile matter, ash content, fixed carbon, and heating value. Crude protein and fat contents were only determined for the random feather category.

The moisture content of feathers was evaluated using an infrared moisture balance; 0.1 g of sample was heated to 105 °C, and the value was recovered directly from the device. Then, the volatile matter was measured by heating under an inert environment. First, clean ground feathers were placed in ceramic crucibles closed by a lid and heated in a calcination furnace (Carbolite, Newtown, PA, USA) to 575 °C until stable mass was achieved. The ash content was measured during the same manipulation as the volatile matter. Next, samples were heated at 575 °C in ceramic crucibles without a lid until stable mass was achieved; ashes were determined as the remaining mass. The fixed carbon content is deduced from Equation (1):

$$Fc = 100 - (Mc + Vc + Ac) \tag{1}$$

where Fc is the fixed carbon, Mc corresponds to the moisture, Vc is the volatile content, and Ac is the inorganic content.

2.3. Theoretical Heating Value

Several theoretical equations predict heating values based on the data obtained from the proximate analysis. One of these studies shows that the heating value is linearly related to the volatile matter, fixed carbon, and ash content [18]. Equation (2) applies to a defined range of constituents, which is 0.92–90.6% volatile matter, 1.0–91.5% fixed carbon, and 0.12–77.7% ash.

$$hv = 0.3536(Fc) + 0.1559(Vc) - 0.0078(Ac) \tag{2}$$

where hv is the heating value.

2.4. Crude Fat Content

Fat content was measured by Soxhlet extraction with petroleum ether (Fisher Chemical, Waltham, MA, USA) at 100 °C for six hours in a Soxhlet extraction system. The recovered fat is then oven-dried and weighed to determine the percentage.

2.5. Protein Content

The Biuret assay verified the presence of protein in duck feathers and quantified using the Kjeldahl method. The determination of proteins by this method is based on the complexation of peptide bonds of proteins by Copper II ions present in the biuret reagent in an alkaline medium. In the presence of proteins, the Biuret reagent (Reagecon) colors a solution in purple. For the analysis, 5 g of ground feathers were dissolved in 100 mL of a 1 mol/L sodium hydroxide (Sigma Aldrich, St. Louis, MO, USA) solution by heating the mixture at 80 °C for 4 h. The resulting solution was filtered and centrifuged to remove all particles and impurities. Then, the Biuret reagent was added to 2 mL of the resulting solution to observe the coloration.

The Kjeldahl method was used to evaluate the nitrogen content of the dry raw feather with an automatic digester (Velp Scientifica DKL8, Usmate Velate, Italy), and an automatic analyzer (Velp Scientifica UDK 159); a conversion factor of 6.25 was used to convert nitrogen content to crude protein content. This factor is based on the fact that most protein contains 16% nitrogen [19]. The dry matter was determined by an infrared desiccator expressed in g/100 g of a raw sample, and the N*6.25 crude protein content was determined in g/100 g of crude sample and g/100 g of dry matter. The analyses were carried out in triplicate.

2.6. Sodium Dodecyl Sulfate PolyAcrylamide Gel Electrophoresis (SDS-PAGE) Analysis

The SDS-PAGE analysis was performed according to the method of Laemmli [20] to compare the raw feather and the extracted keratin. The raw feather was ground to a particle size of 0.08 mm to facilitate its denaturation using Laemmli buffer (Alfa Aesar, Haverhill, MA, USA). The keratin was intentionally extracted from the raw feathers using mild conditions to preserve the molecular weights and enable accurate comparisons. This was achieved by utilizing 907 mM sodium hydroxide (Sigma Aldrich) for extraction, followed by dialysis. In order to establish a reference point, a bovine 2 mg/mL albumin standard (Thermo Scientific, Waltham, MA, USA) was used. All samples, including the raw feather, extracted keratin, and bovine albumin standard, were incubated in $2\times$ Laemmli buffer for five minutes to ensure denaturation. The buffer consisted of 250 mM Tris-HCl (pH 6.8), 8% SDS, 40% glycerol, 8% beta-mercaptoethanol, and 0.02% bromophenol blue.

For the gel preparation, 10 μL of 10–250 kDa Prestained Protein Ladder (Thermo Scientific) was loaded in lane 1, while 10 μL of the feather sample, keratin sample, and bovine albumin standard were loaded in separate wells of the subsequent lanes. The electrophoresis process utilized Bolt™ 4–12% Bis-Tris Plus Gel (Invitrogen™ NW04120BOX, Waltham, MA, USA) and SDS running buffer. The gels were run at 160 V until the dye front reached the bottom of the gel.

Following electrophoresis, the gels were stained with Coomassie Brilliant blue R 250 (Sigma Aldrich) and subsequently rinsed with 5% acetic acid (Sigma Aldrich) and 20% methanol (Fisher Chemical) until a clear background was observed.

2.7. Feather–Solvent Interface

Keratin is an insoluble protein in polar and non-polar solvents with very low chemical reactivity. This test was meant to identify the polarity and stability of random feathers by studying their behavior in individual solvents ranging from highly polar to non-polar, namely water, ethanol (Fisher Chemical), propan-2-ol (Sigma Aldrich), propan-2-one (Fisher Chemical), acetonitrile (Fisher Chemical), toluene (Fisher Chemical), ethoxyethane (Fisher Chemical), trichloromethane (Thermo Scientific), hexane (Fisher Chemical), and pentane. Feathers were placed in every solvent using centrifuge tubes, with a solid-to-solvent ratio of 1:25 (*w:v*).

2.8. Chemical Durability Test

Durability or degradation refers to changes in the physical properties of polymer materials caused by contact with a chemical. For example, a material may change in color, become hard, stiff, or brittle, or become softer, weaker, and swell several times its original size. Various chemicals were used to test the chemical durability of duck feathers (calamus, rachis, and barbs), including cold water, a strong acid consisting of a 1% sulfuric acid (Thermo Scientific) solution with pH 1; a weak acid consisting of 1% acetic acid (Sigma Aldrich) solution with pH 3; a bleaching agent consisting of a 4% Sodium chlorite (Sigma Aldrich) solution; a strong alkali consisting of a 1% sodium hydroxide (Sigma Aldrich) solution with pH $\cong$ 12–13; and a weak alkali consisting of a 0.5% sodium carbonate (Honeywell solution and with a pH of $\cong$10–11. The feather samples (1 g) were placed in covered Petri dishes, completely covered with liquids at room temperature, and then collected after 2 h, 24 h, and 7 days and dried for 24 h. Physicochemical changes were observed.

2.9. Hydrophobicity Test

The hydrophobic behavior of duck feather fractions was compared with known hydrophilic materials, such as cotton fiber and wood pulp, in both an aqueous and an organic solvent phase. The different groups of dried duck feathers and the different parts of the feather (barbs, calamus, and rachis), cotton fiber, and cellulose pulp were soaked in an ethyl–ether–water mixture. Bromothymol blue (Thermo Scientific Chemicals) was used

to color the water to highlight the interface between the two transparent solvents; it was centrifuged in a vortex mixer for 30 s and then allowed to settle overnight.

2.10. Functional Group Analysis by Fourier Transform Infrared (FT-IR) Spectroscopy

Functional groups of ground feathers were analyzed by Fourier Transform Infrared (FT-IR) spectroscopy with an Attenuated Total Reflectance (ATR) mode with a Jasco FT/IR-4700 infrared spectrometer. All spectra have been carried out over a 4000–400 cm^{-1} frequency range using 64 scans and 2 cm^{-1} resolution.

2.11. Pyrolysis–Gas Chromatography/Mass Spectrometry

Pyrolytic degradation products of feathers were analyzed using Py-GC/MS to provide a further comprehensive composition description. The samples were pyrolyzed using a GERSTEL PYRO unit, combined with a thermal desorption unit (GERSTEL TDU) placed on a Cold Injection System 6 (CIS 6) with Controller C506, and connected to a Thermo Scientific Trace 1310 gas chromatograph equipped with a Thermo Scientific ISQ mass spectrometer as a detector. The analysis was conducted utilizing a TG-5SILMS column (30 m × 250 μm × 0.25 μm). Pyrolysis of the samples occurred within a quartz tube housed in a heating chamber under a helium atmosphere. The resulting pyrolysis gas was transferred to the GC system via the heated TDU and CIS unit. Approximately, amounts from 100 to 150 μg of the sample were pyrolyzed at 550 °C for 30 s; before the pyrolysis, the TDU was heated up from 50 °C to 300 °C with a speed of 720 °C/min. After the TDU temperature was reached, the pyrolysis started. The transfer temperature to the CIS module was set to 300 °C. The CIS was used just as an interface to the column of the GC. The temperature of the CIS was set permanently to 300 °C. Helium was the carrier gas at a 1.0 mL/min flow rate. The GC temperature program consisted of the following steps: (i) holding at 50 °C for minutes; (ii) ramping from 50 °C to 220 °C at a rate of 3 °C/min; (iii) holding at 200 °C for an additional 10 min. The mass selective detector was configured to scan the m/z range from 40 to 650. The pyrolysis products were identified by comparing their mass spectra with those stored in the NIST library.

2.12. Thermogravimetric Analysis (TGA)

The thermal resistance of each ground feathers category was measured and conducted in a TA Q2500 thermogravimetric analysis; samples were heated from 30 °C to 800 °C at 10 °C/min under a nitrogen atmosphere.

2.13. Differential Scanning Calorimetry (DSC)

The melting temperatures of all categories were measured using a TA Q20 differential scanning calorimetry under a continuous nitrogen purge at a heating rate of 10 °C/min over a temperature range from −50 °C to 250 °C.

2.14. X-ray Diffraction (XRD)

The crystallinity rate of feathers was measured by Bruker AXS D8 Advanced diffractometer instrument. It was carried out with CuKa radiation (X = 1.542 A) at 30 kV and 15 mA. Data were recorded within the scattering angles range of 5° to 50° at the rate of 0.02°/min. The crystallinity index (CI) was calculated using the Origin software and the following Equation (3).

$$CI\ (\%) = Ac/At \times 100 \tag{3}$$

where Ac is the area of the crystalline domains and At corresponds to the total area under the diffractogram curve.

2.15. Scanning Electron Microscopy (SEM)

Scanning electron microscopy (SEM) was used to study the feather morphology and microstructure. Samples were mounted onto specific stubs and coated with platinum using a

sputter coater (Q150T, Quorum Technologies, Kent, UK). Observations are conducted at 2 kV, in a high vacuum mode, with a Gemini SEM 300 FESEM (Zeiss, Oberkochen, Germany).

2.16. Solid-State ^{13}C CP MAS Nuclear Magnetic Resonance Spectroscopy (NMR)

The solid-state 13C CP MAS NMR spectra of random feathers were recorded at 298 K on a Bruker Avance II 9.4 T spectrometer using a 4 mm rotor with Kel-f cap at 8000 Hz spinning rate. The contact time in the CP MAS experiments was 2.0 ms with a recycle delay of 5 s and 3072 repetitions. Fourier transform was used to process the 1D spectra, and chemical shifts were determined using glycine as an external reference (calibrated on the carbonyl signal at 178 ppm).

3. Results

3.1. Proximate Analysis

3.1.1. Moisture Content

The moisture content reduces the heating value due to endothermic evaporation during heating. As a result, low moisture content yields high heating values. Figure 2 shows the moisture content of the samples. It ranged from 7.65% to 9.91%. The highest moisture content was found in the calamus category, while the lowest was in category 7.
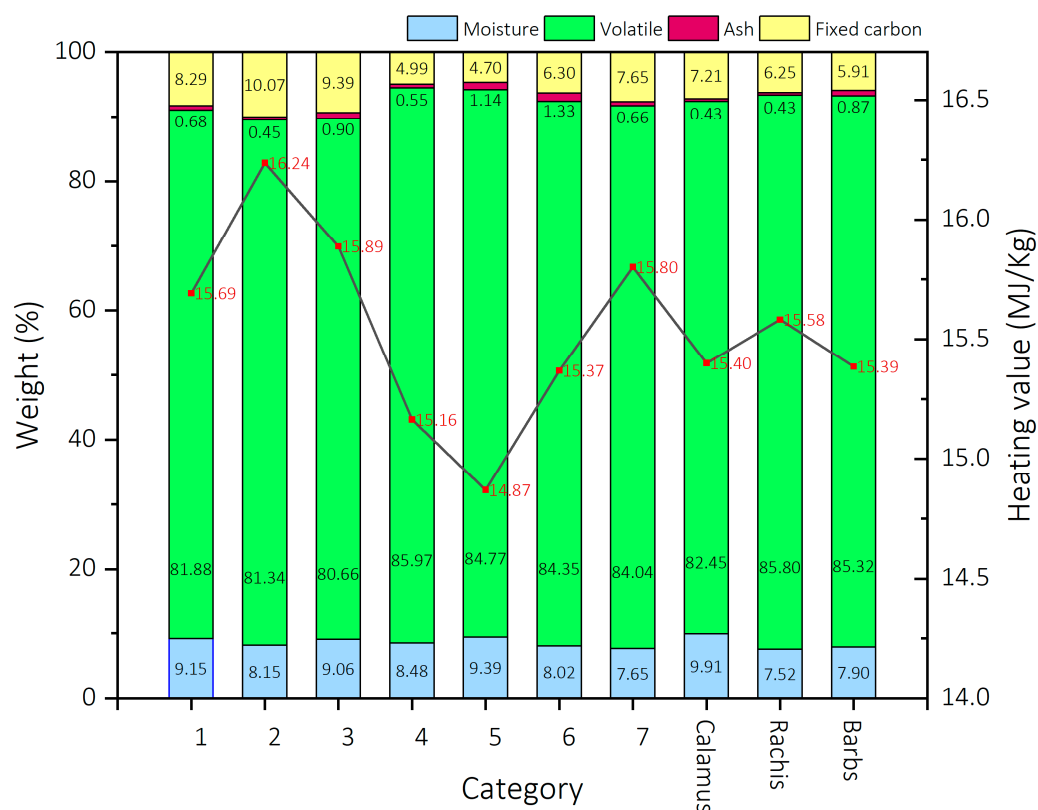

Figure 2. Moisture content, ash content, volatile matter, fixed carbon, and heating value prediction in percentage for duck feathers; the right axis presents the heating value.

3.1.2. Volatile Content

The volatile materials combine methane, hydrocarbons, hydrogen and carbon monoxide, and incombustible gases such as carbon dioxide and nitrogen [16]. Figure 2 showed a high average percentage of volatile matter for the different categories and parts of the feather (80–86%), which are mainly attributed to the light volatile products released during the keratin decomposition, such as CO, CO_2, CH_4, H_2, H_2O, H_2S, HCN, and NH_4 [21,22]. The highest volatile content was found in categories 4, 5, 6, and 7 (85%), which are less mature and contain more barbs than the calamus. Conversely, the lowest values were

found in categories 2 and 3, and, therefore, in random (81%), which had the most of these two categories with a higher calamus weight. This was particularly evident in the calamus, which had the least volatile content compared to the barbs and rachis. Higher volatile matter indicates ease of ignition and rapid burning but low heating values. This indicates that feathers have a good ignition point, removing the excess oxygen demand for a complete burning process.

3.1.3. Ash Content

Depending on the feedstock, the ash level in organic carbon varies greatly [23]. It mainly comprises hydrogen, nitrogen, oxygen, and sulfur [16]. The lower the ash content, the higher the heating value. In Figure 2, it is found that the average percentage of ash was between 0.5 and 1.5% for duck feathers, similar to values previously observed for chicken feathers [16], with the big feathers having approximately the lowest value (0.45%) and the highest heating value of 16.24 MJ/Kg. On the other hand, the smooth feathers (category 6) possessed the highest value of ash (1.33%), resulting in a lower amount heating value (15.37 MJ/Kg). The low ash content for the bigger feathers would allow this waste material to be used for fuel generation with minimal dust emissions and air pollution, thus meeting the requirements for environmentally friendly waste disposal [24]. However, the small and smooth feathers can be preserved for diverse applications, including their use in clothing and as filling material for pillows.

3.1.4. Fixed Carbon Content

The fixed carbon in biomass is the pure combustible component after removing volatile matter. Figure 2 shows that the fixed carbon content of the different categories ranges from 5% to 10%. Big feathers had the highest fixed carbon content, whereas tiny feathers had the lowest. Categories with a higher percentage of fixed carbon content had a relatively higher heating value.

3.2. Theoretical Heating Value

The heating value is the total amount of heat produced during the combustion process of a unit quantity of biomass waste. The higher heating value represents economic utility. According to Parikh's equation, as well as in Figure 2, the hardest feathers in category 2 have the highest heating value of 16.24 (MJ/Kg). As a result, hard feathers with greater calamus and rachis weight hold significant potential for energy production. The utilization of feathers for energy generation proves to be cost-effective and offers advantages such as their widespread availability and minimal need for specialized equipment and infrastructure. This makes feathers an ideal choice for industries in search of renewable and cost-efficient energy sources.

3.3. Crude Fat Content

Feathers were extracted with a Soxhlet to quantify and analyze their fat. Figure 3 shows the FTIR spectrum of the extracted fat. Specific bands can be observed, such as two mediums to strong bands at 2815 and 2848 cm^{-1}, characteristic of the stretching vibrations of methylene (-CH$_2$-) and methyl (-CH$_3$) groups. These two bands can be attributed to representing a long carbon chain typical of hydrocarbons and triglycerides. In addition, a weak band can be observed at 1738 cm^{-1}, which is attributed to the (C=O) bond of ester functions also present in triglycerides and fat [25]. After confirmation of the extracted substance as fat, six extractions were performed, the residues were weighed, and the proportion of fat in the duck feathers was evaluated at 0.98 $\pm$ 0.12%.
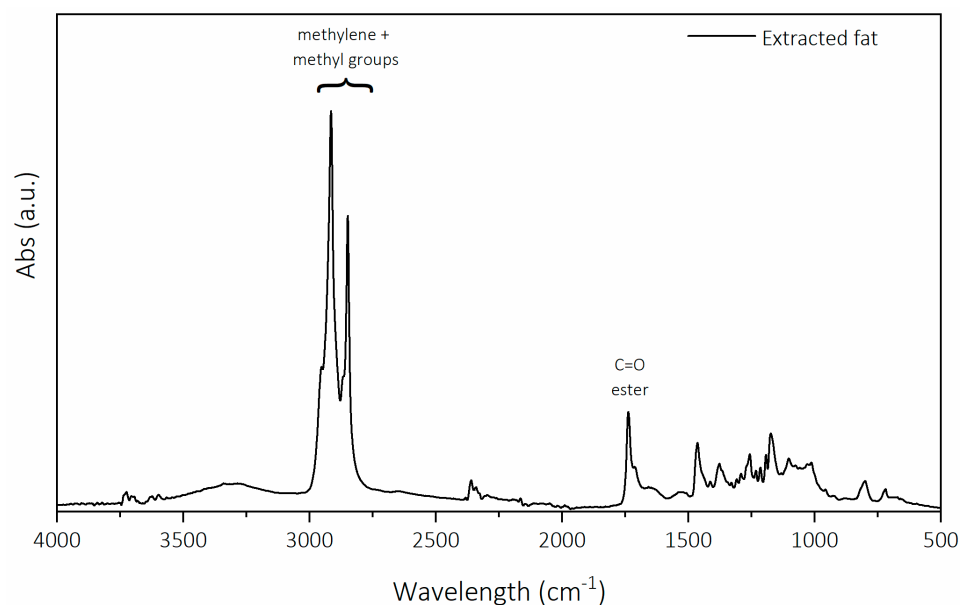
Figure 3. FTIR spectrum of extracted fat from duck feathers extracted using the Soxhlet method.

3.4. Protein Content

The first step in protein analysis was to qualitatively verify the presence of protein in duck feathers. For this purpose, the Biuret method was chosen. After dissolving the crushed feathers in NaOH, the hydrolysate was photographed. Then, the Biuret reagent was added to this hydrolysate to observe a color change. Figure 4 shows two test tubes, the hydrolysate without Biuret on the left and the hydrolysate + Biuret added on the right. A color change from colorless to violet is observed. This violet coloration demonstrates the complexation of peptide bonds of proteins by Copper II ions and proves the presence of proteins in duck feathers. The crude protein content in duck feathers quantified by the Kjeldahl method "N*6.25" was $82.97 \pm 0.98\%$.
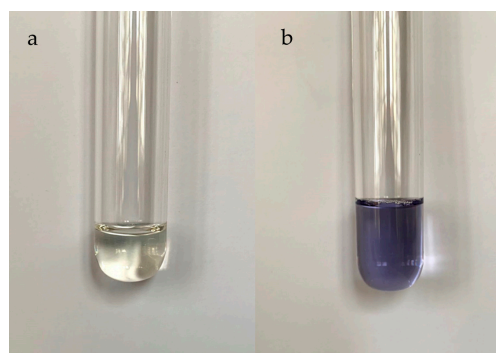

Figure 4. Biuret test; (**a**) before the addition of Biuret reagent, (**b**) after the addition of Biuret reagent.

3.5. Sodium Dodecyl Sulfate PolyAcrylamide Gel Electrophoresis (SDS-PAGE) Analysis

SDS-PAGE gel electrophoresis was used to determine the molecular weight distribution of soluble proteins in both the raw feather material and the extracted keratin. In Figure 5, the raw feather (lane 2) exhibited a distinct protein fraction at approximately 10 kDa, indicating the presence of a feather keratin monomer [26]. Similarly, the extracted keratin, obtained using 907 mM NaOH (lane 3), exhibited a band at 10 kDa, consistent with previous studies [27]. These findings suggest that the molecular weight remains unchanged throughout the regeneration process, implying a stable molecular weight for the keratin in mild extraction conditions. This indicates that the keratin monomers found in the raw feathers are not adversely affected by the extraction process and are likely to remain intact.
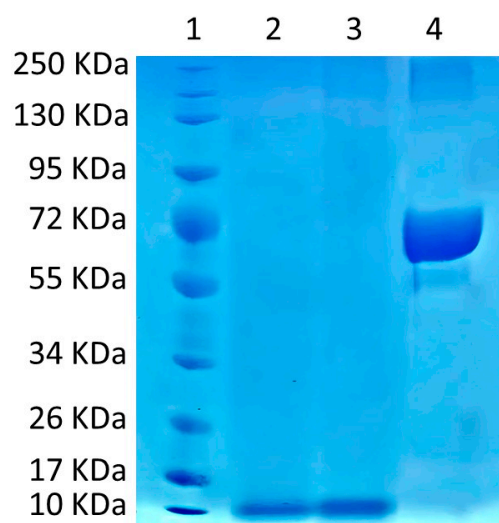
Figure 5. SDS-PAGE of feather hydrolysates, lane (1) Prestained Protein Ladder (10–250 kDa), (2) feather hydrolysate, (3) keratin feather hydrolysate, and (4) albumin standard.

3.6. Feather–Solvent Interface

Solvent effects are relevant to the folding, stability, and dynamics of proteins. As the structural consequences of the honeycomb structure and the disulfide bridges, along with other relevant driving forces that are found in the native keratin tertiary structure, one can gain a better understanding of the hydrophobic and water-repellent properties found in feathers. According to the earliest studies on protein structures, 40–50% of the surface accessible area is made up of apolar groups [28–30]. Furthermore, 30–35% of polar and apolar atom groups are internally buried during folding. As part of this study, the relative contributions of polar and apolar solvents to protein feather solubility and stability were studied by observing the behavior of random ground feathers in five polar solvents (water, ethanol, isopropanol, acetone, and acetonitrile) and five nonpolar solvents (toluene, diethyl ether, chloroform, hexane, and pentane), respectively. These data were used to qualify the strength of internal interactions and the nature of the exposed surface. Figure 6 shows data for the partitioning properties of duck feathers between air and the different solvents. The following trend was: water > chloroform > acetonitrile > toluene > isopropanol > ethanol > diethyl ether > acetone > hexane > pentane. The feather fibers exhibited the most partitioning in air to water and chloroform solvents: this may be because of the high capacity of these two solvents to make hydrogen bonds; on the other hand, acetonitrile is a polar aprotic solvent and possesses a stronger dipole moment than polar protic alcohols and toluene. The feather fractions showed more partitioning in isopropanol than in ethanol. This may be due to a slightly bigger molecule of isopropanol than ethanol providing a hindrance to sorption. On the other hand, diethyl ether can form hydrogen bonds to water, since the oxygen atom is attracted to the partially positive hydrogens in water molecules, making the difference with the polar acetone Moreover, the presence of alkyl groups in feathers makes them hydrophobic in nature; therefore, these hydrophobic chains have a strong affinity toward non-polar solvents such as hexane and pentane. It must be emphasized that the chemical compatibility of materials can be affected by various parameters such as hydrophobicity, lipophilicity, density, pH, temperature, polarity, structure, particle size, and other factors. Despite large uncertainties in the estimates made, it can be concluded that not a single factor dominates the folding process; it is rather a complex combination of hydrophobic, hydrogen bonding, and related entropic effects that are strongly connected through the topology of the molecule producing the important stability of the native structure, making them non-soluble in both aqueous media and nonpolar solvents.

Figure 6. Partitioning properties of duck feathers between air and the different solvents, solvent (1) water, (2) ethanol, (3) isopropanol, (4) acetone, (5) acetonitrile, (6) toluene, (7) diethyl ether, (8) chloroform, (9) hexane, and (10) pentane.

3.7. Chemical Durability Test

Various reactions were observed, including swelling and degradation, color changes, and the time to occur. This test is important to understand the reactivity of duck feathers during manufacturing processes and within a given application. Five groups of chemicals were tested: water, acids (strong and weak), alkalis (strong and weak), and a bleaching agent. Physical changes and chemical degradation are serious problems that can affect natural fibers and materials made from them due to potential swelling and rotting of fibers. Depending on the contact time, feather fractions will suffer varying degrees of damage. According to Figure 7 and Table 2, it can be noted that, in acidic solutions, feathers have mild resistance to weak acids but poor resistance to strong acids. The feathers suffered damage and higher degradation in the tested strong acid than in deionized water. However, bleaching agents can be used safely for bleaching effects, but only for short periods (maximum two hours), as prolonged exposure weakens feathers and causes them to disintegrate. Therefore, using oxidizing solutions such as sodium hypochlorite when cold and diluted and only for a short time, with proper washing after treatment, is important. On the other side, feathers dissolved rapidly in alkaline solutions (both strong and weak alkali). Particularly, barbs have more resistance than the calamus and rachis, where the rachis suffered high weight loss in 1% NaOH after 24 h. These results indicate that duck feathers are unstable in strongly alkaline environments, and these solvents may be used to dissolve feathers easily for keratin extraction processes.

Figure 7. Changes in the physical properties of barbs, calamus, and rachis under different chemical conditions.

Table 2. Observations regarding the physical properties of barbs, calamus, and rachis under different chemical conditions.

	Barbs			Calamus			Rachis		
	2 h	**24 h**	**7 d**	**2 h**	**24 h**	**7 d**	**2 h**	**24 h**	**7 d**
Cold water pH: 5.93	No change	Slightly grey	Softer and grey	No change	Less transparent and softer	Brittle and more matte in color	No change	A little change in color	Degradation with milky dispersion
1% H_2SO_4 pH: 0.96	Slightly yellow	Degradation	Fibers are smaller and yellower	Whiter in color and a little degradation	Softer, mass loss, and more matte in color	Degradation and more white	No change in color, softer	No change in color, softer	Degradation, but no change of color
1% CH_3COOH pH: 3.05	Slightly yellow	Yellower	Yellower	Whiter and a little degradation	Softer, more matte, and intermediate degradation	Whiter, softer, and high degradation	No change	Still very hard, more yellow	Hard and more yellow
4% $NaClO_2$ pH: 11.32	Whiter	Less brilliant and with rose tones	Presence of rose tones	Whiter with a dispersion of particles	More matte and rose	Softer and more rose	Slightly whiter	More rose and softer	Degradation
1% NaOH pH: 12.54	Viscous, immediate swelling, and change to yellow	Yellower	Highly yellow	More matte and yellow	More viscous and yellower	Less yellow and high degradation	Softer and yellower	Softer and more yellow	Degradation with powder dispersion
0,5% $Na_2CO_3H_2O$ pH: 10.75	A little change of color	Grey	More grey	Still transparent	Still hard and more matte	More matte and softer	No change	Softer	Degradation

3.8. Hydrophobicity Test

Hydrophobicity refers to a molecule or particle that avoids water, is uncharged, apolar, incapable of forming hydrogen bonds, or has a low surface energy. There is a range of different methods to evaluate the hydrophobicity of molecules (amino acids, proteins, and detergents) or particles (cells and colloids) [31]. Studies on the ability of preening oil to repel water on smooth surfaces have revealed that duck feathers do not use mainly preening oil for water-repellent characteristics [32], but instead, they have a highly ordered, hierarchically branched multi-scaled structure that provides them with a proper surface roughness for water repelling [33]. According to the principles of superhydrophobicity [34–36], the increase of the surface roughness of solid surface results in the increase of the water contact angle, which is usually used to evaluate the wettability of solid surfaces. The surface of duck feathers can be regarded as heterogeneous surfaces composed of solids and air.

In general, charged groups are fully exposed to the solvent, but, here, this is not the case; covalent bonds such as internal disulfide bridges are formed between pairs of cysteyl residues, with the local neighborhood of the buried charge containing several water molecules, which act as a dielectric effect to reduce the destabilizing effects of an unbalanced internal charge [37,38]. In addition, the hydrophobic interactions between nonpolar residues also have a dielectric effect, which provides the largest single contribution to protein stability [39]. Hence, the exposure of polar groups is strongly related to the number of internal hydrogen bonds, explaining the dominance of a hydrophobic driving force. As shown in Figure 8, cotton and wood pulp were aggregated in the water layer, demonstrating their complete wettability, while the feathers of all groups and different parts (barbs, calamus, and rachis) were gathered between the interphase of water and ethyl ether. This result is explained by the multi-scaled structures on duck feathers, making them super water repellent, in contrast to the hydrophilic cotton fiber and cellulose pulp; this

observation supports the hydrophobic characteristics of duck feathers and broadens their potential applications.
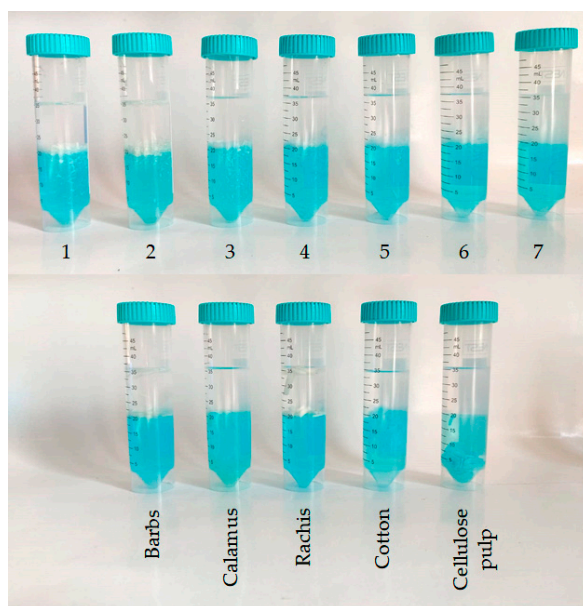

Figure 8. Hydrophobicity test on the different categories of duck feathers, including barbs, calamus, rachis, cotton, and cellulose pulp.

3.9. Functional Group Analysis by Fourier Transform Infrared (FT-IR) Spectroscopy

The chemical structure of each sample was studied with FT-IR, and the spectra are compared in Figure 9; moreover, Figure 10 contains the FT-IR spectra of the different feather fractions. First, it can be observed that the spectra have the same characteristic bands between categories and between feather fractions. Moreover, the results obtained are similar to the results present in the literature concerning chicken feathers [16,40,41]. Therefore, we can deduce that duck feathers do not chemically differ significantly from chicken feathers. In the infrared analysis of the proteins, characteristic bands generated by the general backbone of the proteins were found. Here, the bands visible on the spectra relate to Amide A, Amide I, Amide II, and Amide III [42]. The broad peak at 3300–3200 cm^{-1} is attributed to Amide A. This band comes from the stretching vibration of the NH bond, and its frequency depends on the strength of the hydrogen bond [43]. The highest band at 1700–1600 cm^{-1} is assigned to the absorption of Amide I. This band is caused by the vibration of the C=O bond in the peptide group coupled with slight in-plane NH bending [42,44]. Estimating the secondary structure of proteins is possible thanks to the analysis of the Amide I band, which is closely correlated to this secondary structure. Molecular geometry and hydrogen bonding patterns give rise to different frequencies for the same band. Indeed, the Amide I band is a superposition of different bands corresponding to structures such as α-helix and β-sheet. A deconvolution of the band makes it possible to know the proportion of each structure [42]. The Amide II is found with the band at 1550–1500 cm^{-1}, which is smaller than the Amide I. It is due to the bending of the N-H bond in the plane and to the vibration of the C-N [42]. At 1300–1200 cm^{-1}, a weaker band corresponds to Amide III. The determination of this band is complex due to its position and the contribution of several phenomena and bonds. Indeed, it is often attributed to the C-N vibration coupled with the bending of N-H [16], but absorption can be supplemented by CH$_2$ wagging vibrations in this region [45].
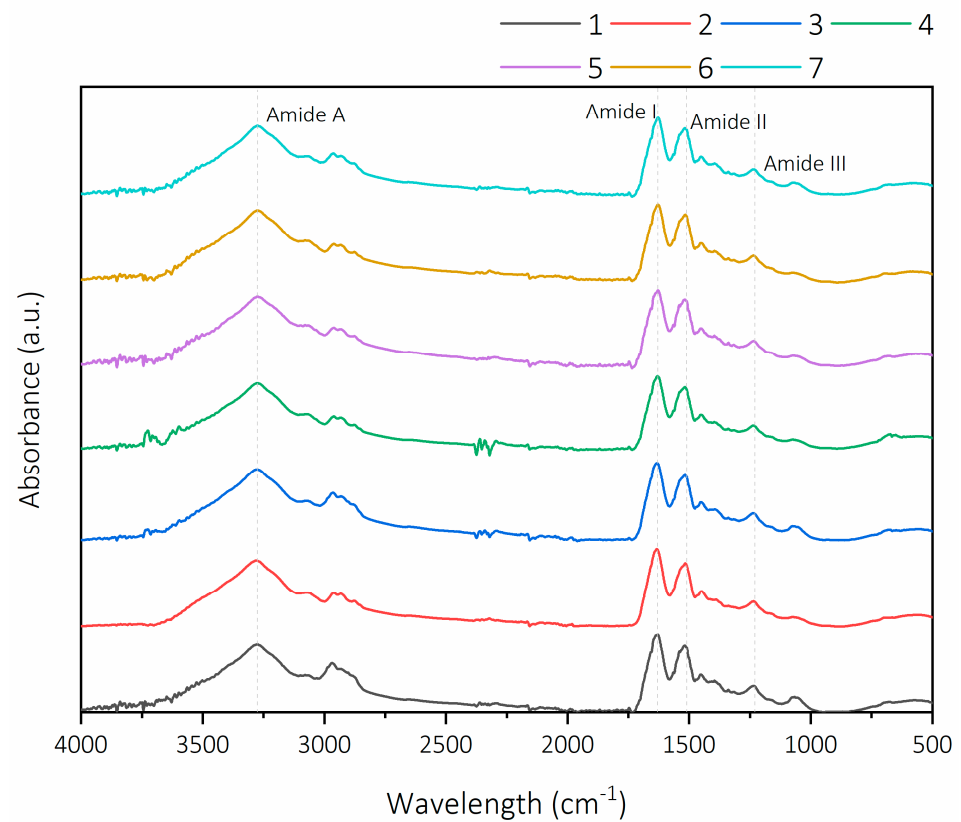
Figure 9. Comparison of FT-IR spectra of duck feathers. Top: each category; bottom: different parts of the same category.
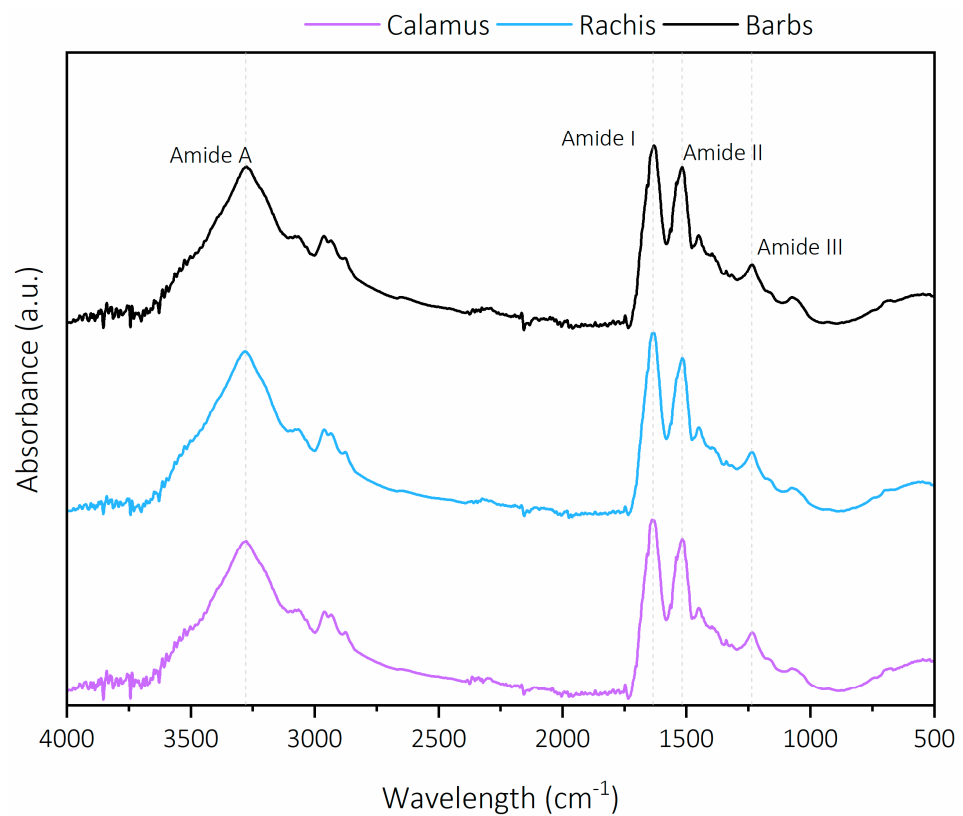

Figure 10. Comparison of FT-IR spectra of duck feathers, top: each category; bottom: different parts of the same category.

3.10. Pyrolysis–Gas Chromatography/Mass Spectrometry

The Py-GC/MS pyrograms of duck feathers revealed a diverse array of degradation products, as summarized in Table 3. The mass spectrum in Figure 11 exhibits a sharp peak at retention time $\cong$ 4 min, corresponding to toluene. Pyrolysis of duck feathers resulted in the formation of numerous nitrogen-containing compounds (amines, amides, nitriles, pyrazoles, pyrroles, and pyrazines) and sulfur-containing compounds (sulfides, thiophenes, and isocyanides). These compounds often contain hazardous or toxic moieties such as sulfur, cyanide, and benzene.
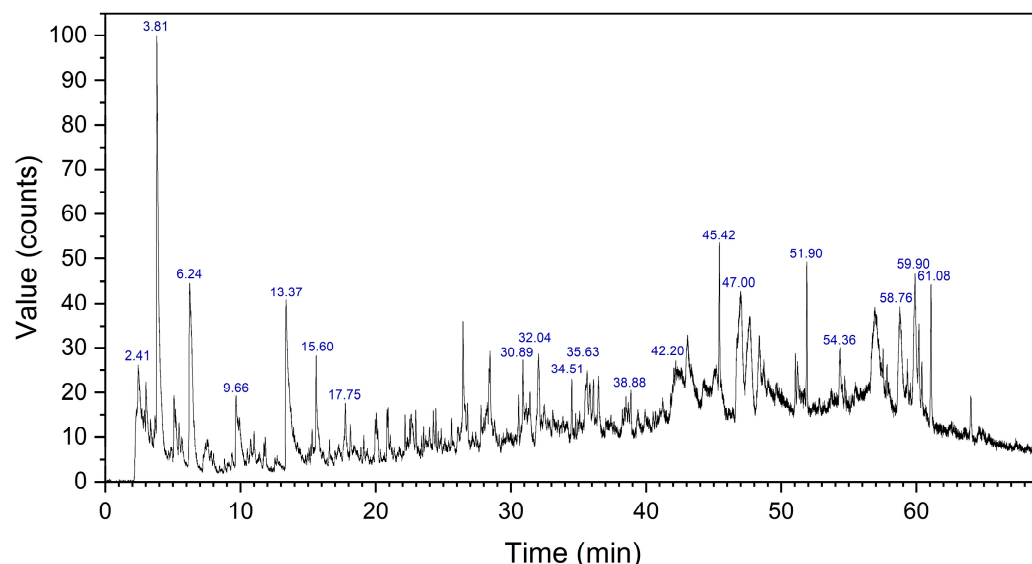

Figure 11. Py-GC-MS chromatogram of duck feathers.

The wide range of obtained pyrolysis products is unique and specific to the precursors, confirming the identity of major amino acids or fatty acids in feathers. The nitrogen-containing compounds originated from the amino acids found in keratin protein and provide valuable information about the amino acid composition and structure of the original feather material. By analyzing the different structures of compounds formed during pyrolysis (side chains, functional groups, ring structures, etc.), valuable insights into the properties of the precursors can be obtained, as indicated in Table 3.

Prominent derivatives of cysteine, proline, phenylalanine, leucine, and histidine in the pyrolysates confirm that these amino acids are major components of feather keratin. The sulfur-containing compounds are more likely to be derived from cysteine and methionine. Cysteine's thiol group is susceptible to various redox reactions, disulfide bond formation, cyclization reactions, and other chemical modifications, making it more reactive compared to other amino acids. Methionine, on the other hand, contains a thioether group ($-S-CH_3$) in its side chain, which is generally less reactive but can still undergo certain chemical modifications, especially under oxidative stress conditions, leading to the formation of reactive species such as sulfoxides or nitriles.

Detecting toxic compounds such as carbonyl sulfide, phenol, m-Cresol, tropilidene, cyanides, and nitriles implies that incomplete combustion presents potential hazards. Additionally, the presence of palmitonitril and palmitamide indicates the degradation of hexadecanoic acid, while icosanenitrile likely originates from icosanoic acid, both lipids in feathers.

Table 3. Analysis of different compounds found in chicken feather barbs with Peak identification according to NIST library.

Apex RT	Start RT	End RT	Area	%Area	Height	%Height	Potential Name	CAS	RSI	% Probability	Amino-Acid
2.41	2.19	2.41	10,217,944.3	1.34	1,216,886.09	1.72	Carbonyl sulfide	463-58-1	959	43.16	Cysteine
3.01	2.99	3.24	6,502,024.97	0.86	934,414.229	1.32	3-Pyrroline	109-96-6	822	17.79	Proline
3.82	3.73	4.51	89,308,181.4	11.75	7,800,103.03	11	Tropilidene = 1,3,5-cycloheptatriene	544-25-2	884	22.15	Unknown
5.09	5.01	5.18	7,035,543.03	0.93	1,202,476.91	1.7	Isoamyl cyanide	542-54-1	856	81.56	Cysteine
5.2	5.19	5.39	4,261,249.52	0.56	812,735.278	1.15	2-Methylpyrrole	636-41-9	788	48.66	Threonine
6.24	6.17	6.71	48,787,578.5	6.42	3,204,032.84	4.52	Annulene	629-20-9	903	41.83	Unknown
8.02	7.95	8.1	1,347,111.09	0.18	273,960.67	0.39	2-(benzylamino)-Ethanol	104-63-2	802	19.72	Phenylalanine
8.45	8.4	8.51	432,117.49	0.06	148,100.749	0.21	1-Pyrrolidinacetonitril	29134-29-0	712	23.23	Proline
8.81	8.75	8.91	1,045,985.54	0.14	254,387.344	0.36	4-Ethyl-2-Methyl-1H-pyrrole	5690-96-0	757	11.11	Leucine
9.37	9.3	9.46	1,360,422.97	0.18	243,607.197	0.34	1-Ethyl-2-Pentylcyclopropane	62238-08-8	838	10.72	Valine
9.66	9.6	9.87	13,611,271.7	1.79	1,264,273.21	1.78	Phenol	108-95-2	822	21.63	Tyrosine
11.74	11.69	11.8	1,669,514.18	0.22	402,848.019	0.57	Limonene oxide	4959-35-7	623	11.87	Unknown
11.83	11.81	11.94	2,685,717.76	0.35	629,397.282	0.89	Pyrrole-3-butyronitrile	874-91-9	727	15.53	Cysteine
13.37	13.31	13.88	50,337,462.2	6.62	2,993,103.56	4.22	m-Cresol	108-39-4	865	30.77	Tyrosine
15.29	15.25	15.36	1,788,578.54	0.24	450,982.12	0.64	3-Methyl-1H-Pyrazol-4-amine	NA	755	37.76	Histidine
15.6	15.55	15.71	9,237,260.71	1.22	1,768,648.09	2.49	o-Tolylisocyanide	10468-64-1	842	20.19	Phenylalanine
17.75	17.69	17.87	5,245,694.99	0.69	938,328.249	1.32	1,1,2,3-Tetramethylcyclohexane	6783-92-2	767	7.25	Leucine
18.12	18.08	18.26	2,885,956.51	0.38	583,139.227	0.82	2,6-Dimethyldecane	13150-81-7	793	10.57	Leucine
18.91	18.84	18.97	926,986.122	0.12	247,447.628	0.35	N-Vinyl-2-pyrrolidone	88-12-0	764	74.06	Proline
19.12	19.08	19.2	1,299,226.6	0.17	383,174.285	0.54	6,7-Dihydro-4H-tetrazolo [1,5-a]pyrimidin-5-one	NA	633	29.65	Histidine
19.97	19.93	20.01	2,568,021.18	0.34	687,111.613	0.97	3-Phenylproprionitrile	645-59-0	853	45.25	Phenylalanine
22.17	22.11	22.23	2,357,982.19	0.31	673,214.156	0.95	Cyclotridecane	295-02-3	818	5.28	Unknown
22.64	22.58	22.8	5,908,475.42	0.78	662,919.761	0.94	5H-1-Pyrindine	270-91-7	868	42.7	Histidine
22.96	22.92	23.04	2,712,484.68	0.36	697,079.157	0.98	N-Allyl-1-1aziridnecarboxamide	30530-01-9	762	50.27	Serine
23.39	23.33	23.45	1,334,877.14	0.18	397,531.214	0.56	Cyclobutanone, oxim	2972-05-6	865	60.45	Proline
24.45	24.41	24.5	1,987,654.55	0.26	683,373.916	0.96	3,56-Diazohomoadamantan-9-one	126126-45-2	608	19.03	Unknown
30.58	30.49	30.62	2,320,396.36	0.31	715,367.162	1.01	1-Hydrocyclodecanecarbonitrile	882-83-7	709	3.52	Cysteine
30.89	30.8	31.51	17,335,673.5	2.28	1,333,680.93	1.88	2,6,10,15-Tetramethylheptadecane	54833-48-6	723	8.67	Unknown
32.04	31.84	32.2	13,240,315.7	1.74	1,404,982.68	1.98	3,3′-Tertramethylenebis(2-oxo-1,3-oazolidine)	91005-98-0	554	10.53	Unknown
34.51	34.45	34.55	2,455,711.36	0.32	832,483.357	1.17	10-Heneicosene	95008-11-0	838	3.5	Unknown
35.63	35.42	36.19	21,283,538.5	2.8	983,209.885	1.39	Hexahzdropyrrolizin-3-one	126424-83-7	695	23.3	Proline
38.88	38.79	38.93	3,262,824.64	0.43	659,253.54	0.93	2,4,4-Trimethyl-3-(3-oxobutyl)cyclohex-2-enone	72008-46-9	585	14.29	Unknown
39.4	39.2	39.62	4,589,236.9	0.6	441,207.251	0.62	3-[(2E)-2-Butenyl]thiophene	53966-44-2	641	5.97	Methionine
42.2	41.91	42.81	21,148,967.5	2.78	733,781.531	1.04	Hexahydropyrrolo [1,2-a]pyrazine-1,4-dione	19179-12-5	767	21.22	Proline
45.42	44.89	45.77	26,838,322.1	3.53	2,905,599	4.1	Hexadecanenitrile	629-79-8	748	15.48	Hexadecanoic acid
47	46.53	47.22	48,940,750	6.44	2,118,489.89	2.99	3-Isobutylhrxahydropyrrolo [1,2-a]pyrayine-1,4-dione	5654-86-4	748	86.31	Leucine
51.9	51.82	51.96	10,502,814.2	1.38	2,634,405.55	3.72	Eicosanonitrile	4616-73-3	721	25.5	Icosanoic acid
54.36	54.24	54.56	8,359,922.5	1.1	994,112.793	1.4	Palmitamide	629-54-9	711	46.5	Hexadecanoic acid
58.76	58.59	59.07	23,080,982.3	3.04	1,585,611.64	2.24	Pyrrolo [1,2-a]pyrazine-1,4-dione, hexahydro-3-(phenylmethyl)-	14705-60-3	813	68.51	Tryptophan
59.9	59.67	60.48	44,684,442.7	5.88	2,441,789.35	3.44	Pyrrolo [1,2-a]pyrazine-1,4-dione, hexahydro-3-(phenylmethyl)-	14705-60-3	813	68.51	Tryptophan
61.08	60.99	61.15	11,398,521	1.5	2,433,167.39	3.43	trans-2,3-Diphenylcyclopropylmethyl Phenyl Sulfide Sulfoxide	131758-71-9	679	31.87	Methionine

3.11. Thermogravimetric Analysis (TGA)

The thermal stability of each feather category was obtained using a TGA analysis. The comparison of the curves of the seven categories and each part can be found in Figure 12, while that of the three main feather sections is presented in Figure 13. Each curve follows the same trend with a pattern of two stages of degradation. First, a small percentage of mass loss occurs up to 100 °C, which is attributed to the evaporation of the hydrogen-bonded water present in the sample. This mass loss is about 8–9%, which agrees with the moisture value of the feathers previously determined. The main degradation of the material occurs from 230 °C with a substantial degradation until around 500 °C. During this step, 70% of the mass is degraded, and this is attributed to the denaturation of the structure and the breakage of peptide bonds between chains as well as the disulfide bridges, which generally degrade from 230 °C and release an H_2S volatile compound [46]. Beyond this temperature, the material degrades almost wholly. A slight difference is observed with the curve of category 7, which represents the down curve. The final mass of this sample is lower than that of the other categories, at approximately 15%, which shows that the down curve has more tendency to be degraded by the temperature. Concerning the barbs, rachis, and calamus, the curves are similar to the previous explanations, with the same stages of degradation and the same losses of mass. No difference is observed depending on the parts of the same feather category.
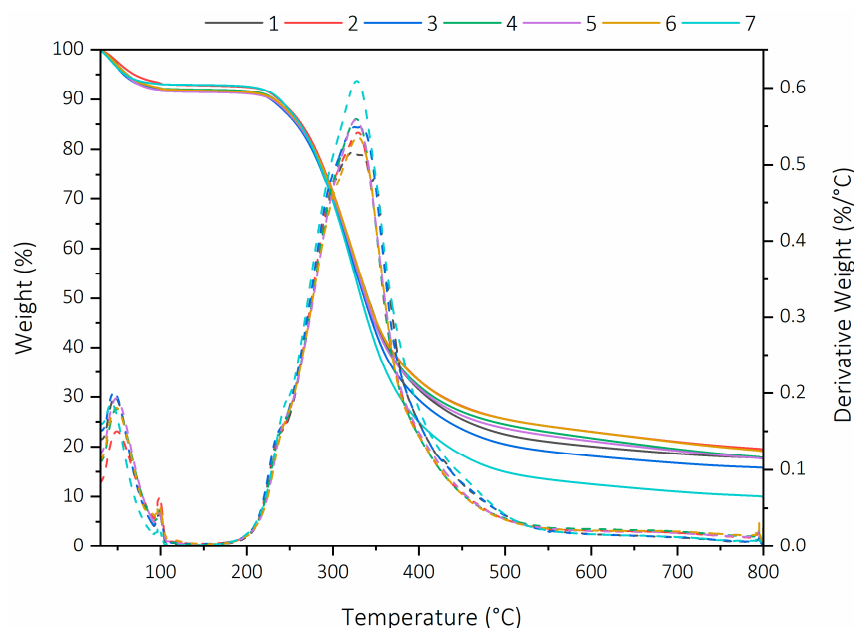

Figure 12. Comparison of TGA and dTG curves of each category of duck feathers.

3.12. Differential Scanning Calorimetry (DSC)

DSC studied the thermal transitions of the feathers. The melting temperature (T_m) was investigated for all categories and fractions to know the differences in thermal resistance according to the morphology of the feathers (hard or soft parts). The resultant curves are shown in Figure 14 (types of feather) and Figure 15 (feather sections). Each curve broadly shows the same trend, with a main endothermic peak around 230–245 °C representing a fusion. This refers to melting the protein crystal structure and the degradation of the a-helix structure and cystine decomposition [47]. However, a closer look shows a slight temperature difference between categories 1, 2, 3, 4, and, 5, 6, and 7. For the first four categories, the melting peak is at 230–235 °C; for the last three categories, the melting temperature is higher (245 °C). This difference is also found on the curves of the three fractions of feathers between the rachis, barbs, and calamus. Indeed, the calamus and rachis have a melting peak at 230–235 °C while that of the barbs is at 240 °C. These results are coherent, considering the composition of each category. Indeed, categories 1, 2, 3, and

4 contain hard parts (rachis and calamus) in a higher quantity than categories 5, 6, and 7, which are soft feathers and mainly composed of barbs. Moreover, this difference in T_m can be due to a difference in crystallinity within the various fractions of the feather because the more the temperature of fusion is raised, the crystallinity of the material is big, conversely [48].
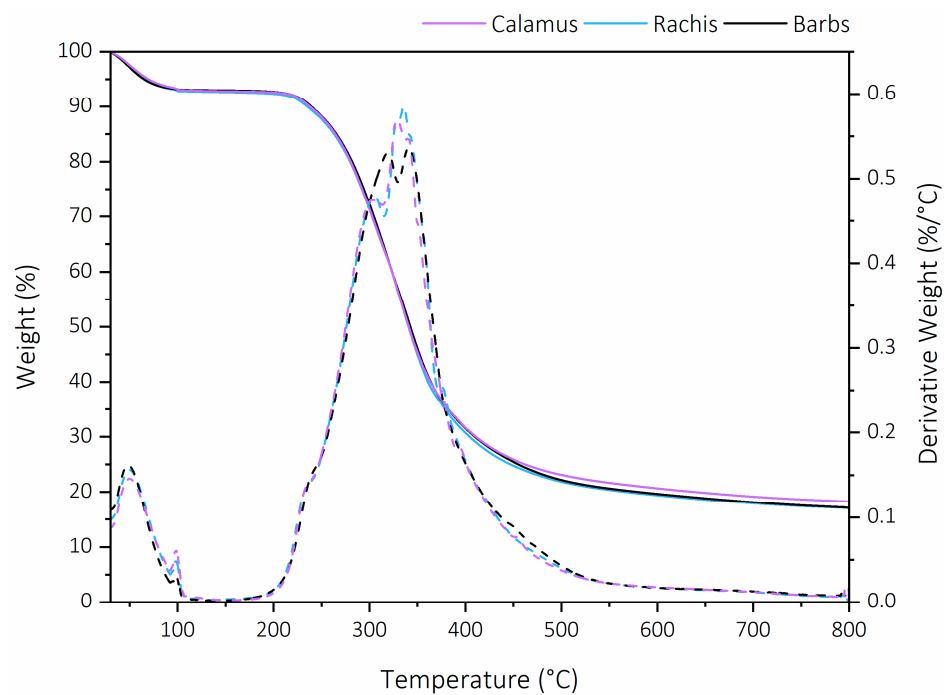

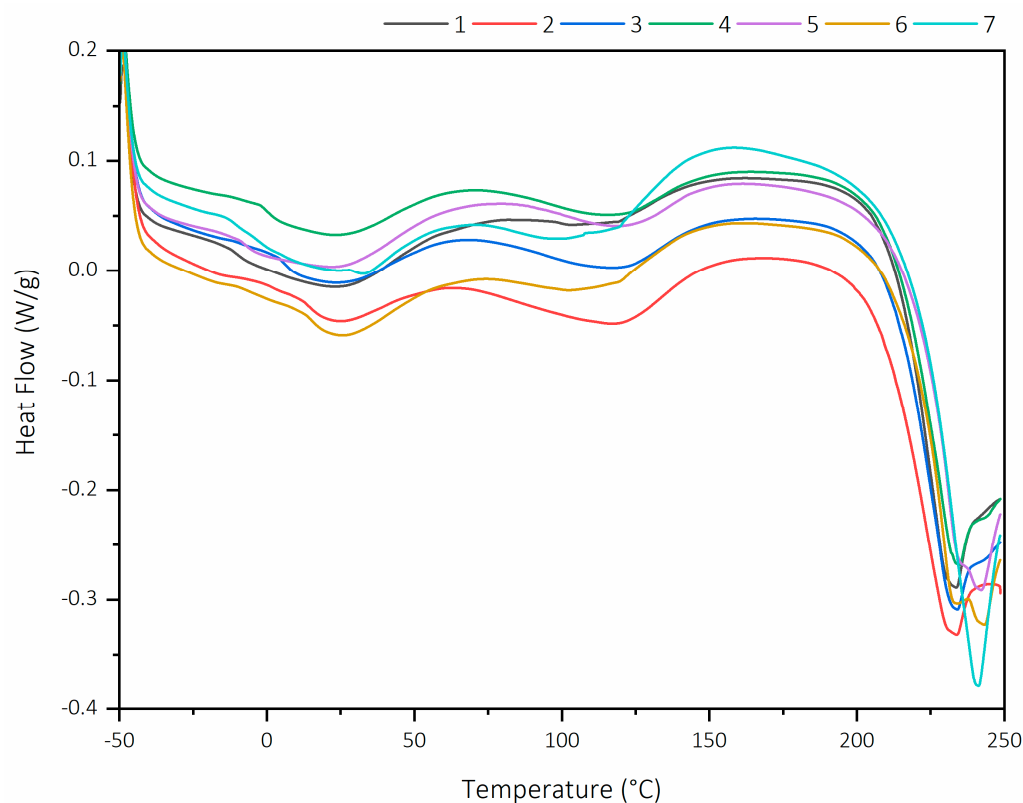**Figure 13.** Comparison of TGA and dTG curves of duck feather fractions.

Figure 14. Comparison of DSC curves of each category of duck feathers.

Figure 15. Comparison of DSC curves of feather fractions.

3.13. X-ray Diffraction (XRD)

Crystallinity defines the degree of order in a material. The more crystalline a polymer is, the more its chains are regularly aligned. Increasing the degree of crystallinity increases hardness and density and can influence their physicochemical and thermal properties. XRD patterns of each type of feather and the feather fractions were investigated. As presented in Figures 16 and 17, all categories and feather fractions exhibit similar diffraction patterns. The appearance of the curves allows us to confirm that the feathers have a semi-crystalline structure by the presence of two peaks at about $2\theta = 9°$ and $2\theta = 19°$, corresponding, respectively, to α helix and random coil + β-sheet [49] structures, including amorphous regions around crystal peaks. Considering that the intensity of a peak is relative to its proportion in the material, it can be observed that the second peak corresponding to the random coil + β-sheet structure is predominant compared to the weaker peak assigned to the α-helix structure. This means that the majority of the structure in the feathers is the random coil + β-sheet structure, confirming the literature [50–52]. All crystallinity rates and calculated α-helix and random coil + β-sheet structure percentages are shown in Table 4. The crystallinity rates range from 52.15% to 60.90%, with a rate of 57.26% for the random category, chosen as an average value for the duck feathers studied in this work. For the different parts composing the feather (Figure 17), the rachis and the calamus had lower crystallinity indices (53.05%, 54.63%), while barbs had the highest (55.21%). Logically, as the number of barbs in a feather increases, so does its crystallinity. These results are consistent with the DSC curves presented earlier, which show that the melting temperature of barbs is slightly higher than that of rachis and calamus due to their higher crystallinity rate, which requires more energy to melt the crystal lattice. Moreover, the results confirm that the random coil + β-sheet structure is the majority structure in the feathers, as its proportion varies from 63.35% to 69.15%, while the α-helix structure is present only between 30.85% and 36.65%.
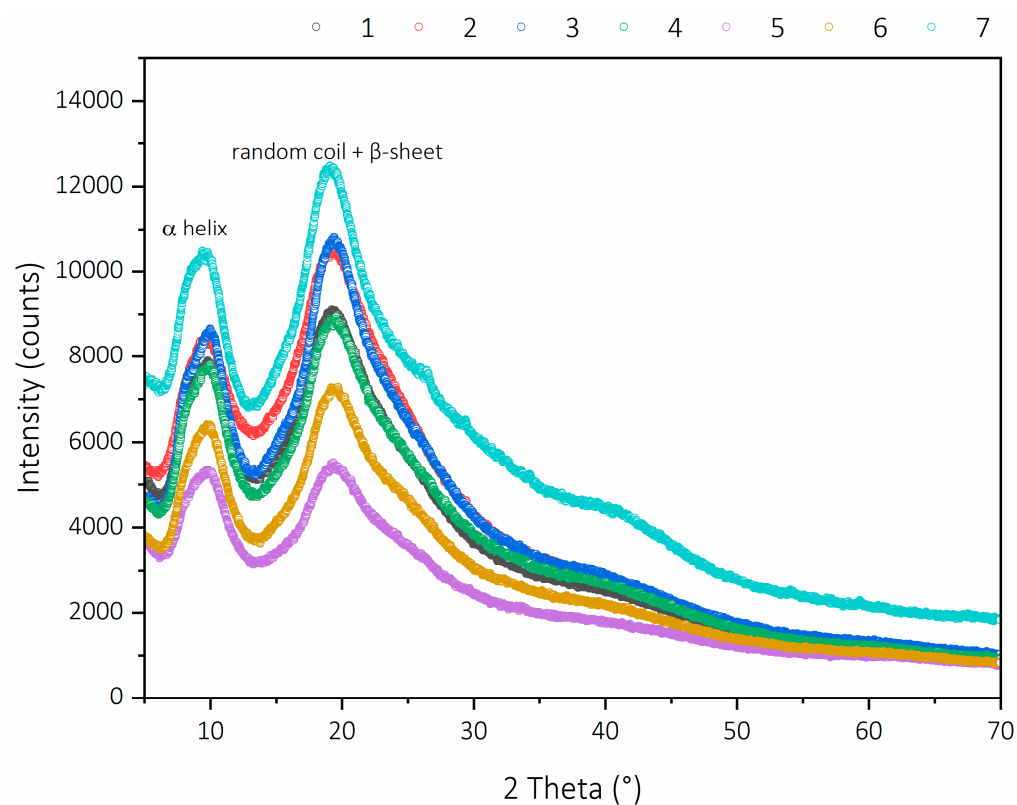
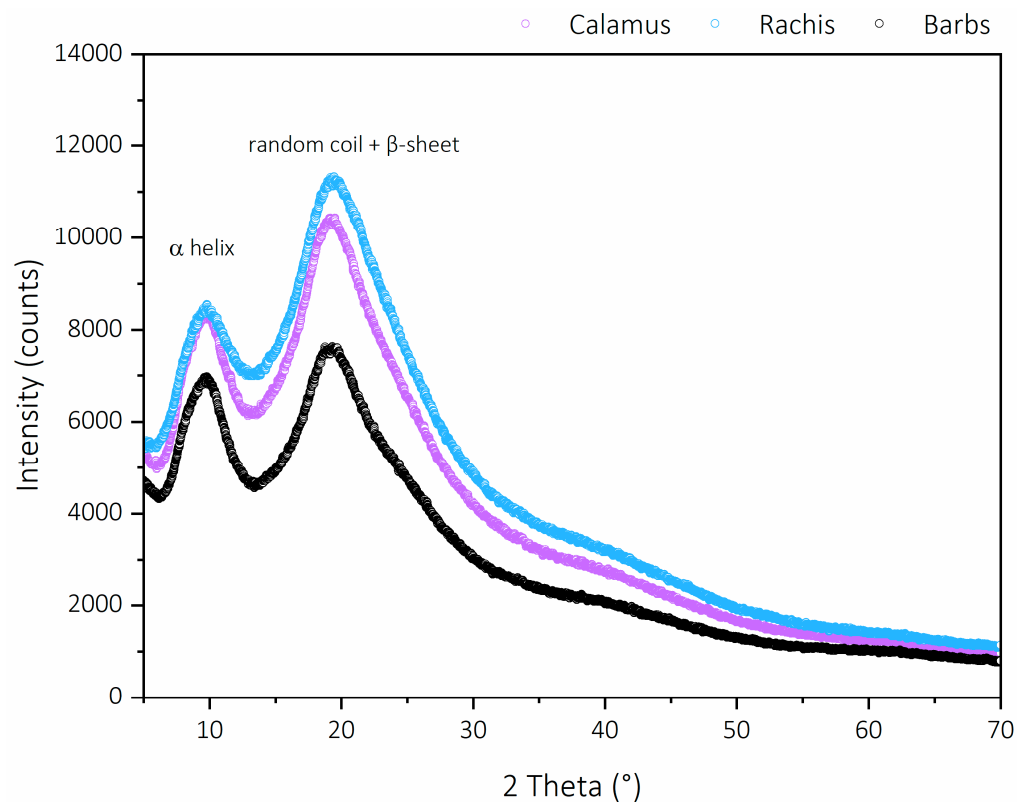**Figure 16.** Comparison of XRD curves of duck feathers.

Figure 17. Comparison of XRD curves of different parts of the feather.

Table 4. Crystallinity rates of the different feather categories calculated from XRD patterns.

Category	Crystallinity Rate (%)	α-Helix Structure (%)	Random Coil + β-Sheet Structure (%)
1	57.26	31.56	68.44
2	53.64	31.69	68.31
3	54.03	31.98	68.02
4	56.14	33.01	66.99
5	60.90	31.22	68.78
6	57.42	36.65	63.35
7	52.15	32.71	67.29
Barbs	55.21	36.55	63.45
Rachis	53.05	30.85	69.15
Calamus	54.63	31.27	68.73

3.14. Scanning Electron Microscopy (SEM)

A feather's main function is protecting and enabling the animal to fly. These functions can be fulfilled thanks to the specific structure of the feathers. SEM and the images observed the morphological characteristics of the different parts of a feather and are presented in Figure 18. Each part, the barbs, the rachis, and the calamus, was observed at a magnification of ×500 and ×3000. First, there are three hierarchical levels in the morphology of the feather. The rachis is the main shaft attached to smaller branches called barbs. These barbs are arranged in parallel to each other, forming a highly ordered structure. On these barbs, on a smaller scale, we can identify other branches, called barbules, which are thin and end in hooklets or with a flatter and wider shape. This hierarchical structure of feathers was previously demonstrated in the study of Kovalev et al., who show that these hooklets maintain the integrity of the feather through an "unzipping" effect by holding on to each other. As a result, barbules and barbs can be separated and then reattached thanks to these hooklets [53]. The cross-section of the rachis reveals two distinct structures. The outer tube is composed of a compact and non-porous material, while the inner tube is filled with a non-compact and honeycomb-like foam structure. On a smaller scale, it can be observed that the walls of these cells are made up of fibers that form a porous structure. This honeycomb structure makes the feathers light but extremely strong [54]. The calamus is the empty part of the main shaft that is directly connected to the animal in its skin. The images show that its inner or outer structure is flat and quite smooth. However, the images show overlapping thin layers leading to rougher structures. Cracks and indentations in the image also show that exposure to the environment may damage the outer calamus.

3.15. Solid-State ^{13}C CP MAS NMR

The solid-state NMR spectrum of the random category was obtained to determine its chemical composition and is shown in Figure 19. The peak with the highest intensity is at 174 ppm and is assigned to the amide carbonyl carbon (C=O) and the random coil + β-sheet molecular structure of keratin [55]. The peak at 131 ppm is representative of aromatic carbons [56]. The spectral region around 50–60 ppm is due to the α-carbon and the peak at 44 ppm is representative of the β-carbon present in leucine and in cross-linked cysteine residues, which are involved in keratin's intermolecular disulfide bridges [57,58]. The complex line shape at around 20–30 ppm is due to the carbon resonance of the alkyl groups of the side chains [59].
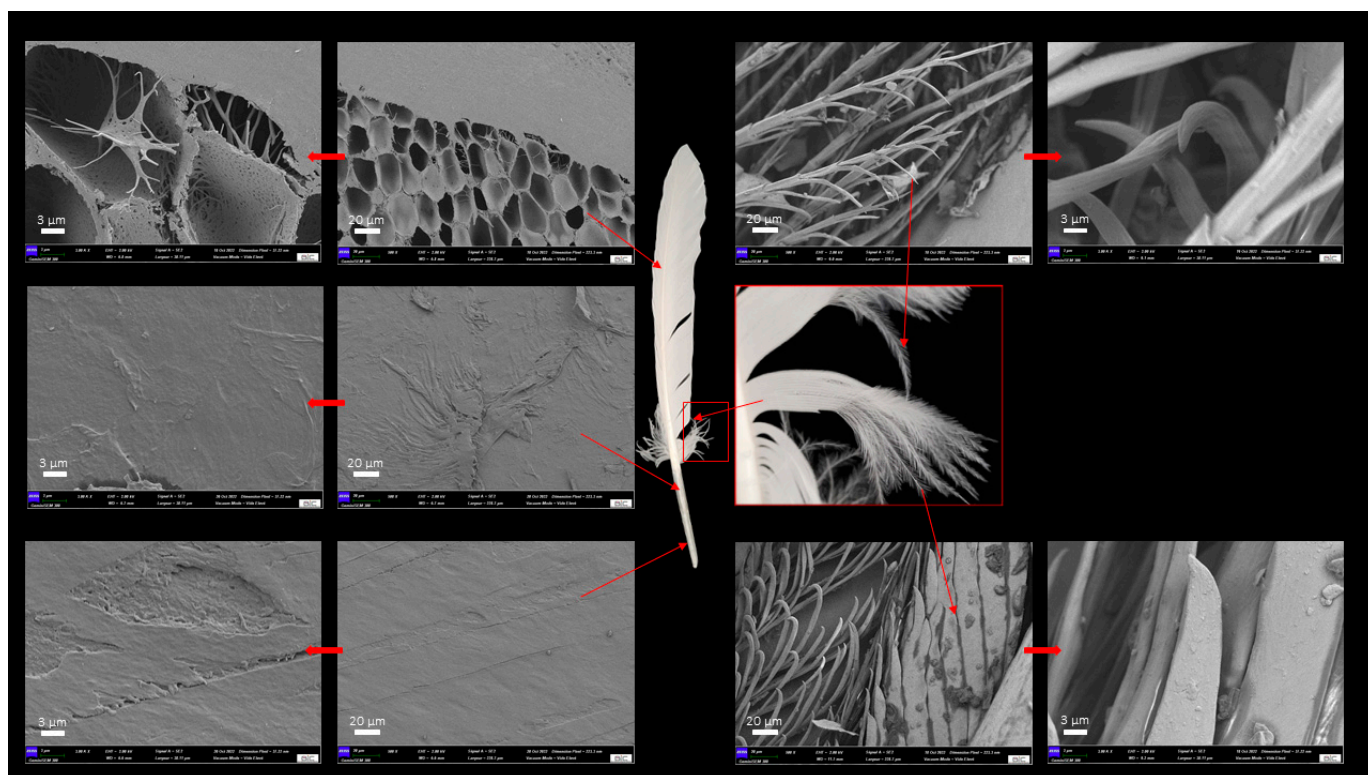
Figure 18. SEM images of different fractions of duck feathers: Barbs, barbules, rachis, calamus in, and calamus out. Central images correspond to 500 magnifications, while external ones correspond to 3000 magnifications.
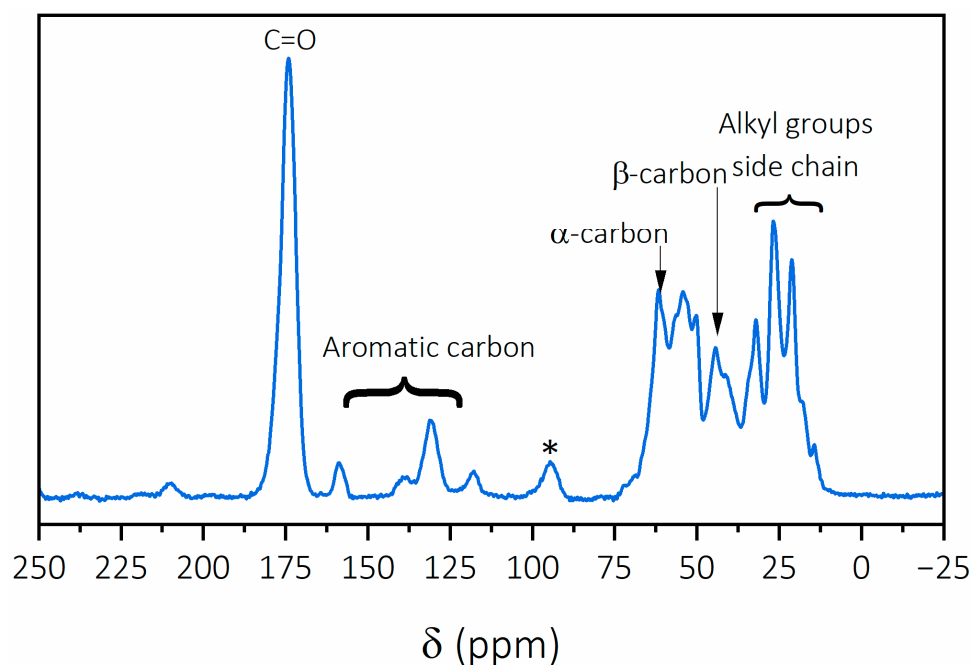

Figure 19. Solid-state ^{13}C CP MAS NMR spectrum of random feather category. The spinning band is noted by *.

4. PhysicoChemical Properties of Duck Feathers and Their Potential Value

4.1. High Keratin Content

Keratin-based products can include producing keratin-based cosmetics, hair care products, skincare formulations, wound dressings, fertilizers, soil amendments, animal

feed supplements (feather meal), biomedical applications, drug delivery systems, wound healing dressings, and biocompatible coatings for medical devices.

4.2. Heating Value

Feathers' high heating value opens up opportunities for energy production, biomass fuel applications, waste-to-energy conversion, industrial heat generation, and the development of value-added products. For example, feathers with a high heating value can be processed into activated carbon. This finds applications in water purification, air filtration, and gas adsorption. By harnessing this heating value, feathers can be effectively utilized as a valuable and sustainable resource. This will contribute to the circular economy and reduce environmental impacts.

4.3. Hydrophobicity

By harnessing feather hydrophobicity, innovative materials and technologies can be developed for a range of applications. These include waterproofing, absorption, moisture management, self-cleaning surfaces, microfluidics, and surface coatings. These applications offer benefits such as improved performance, reduced environmental impact, and increased durability in various industries.

4.4. Honeycomb Structure

By leveraging the advantages of the honeycomb structure in feathers, innovative materials and designs can be developed for lightweight construction, impact resistance, thermal insulation, sound absorption, fluid dynamics, filtration, and packaging. These applications offer benefits such as improved performance, energy efficiency, noise reduction, and protection in various industries and everyday use cases.

4.5. Fiber Structure

Taking advantage of feather fiber structure, innovative materials and products can be developed for strength, durability, flexibility, elasticity, and moisture management. Feather fibers have high tensile strength, making them resistant to breaking or tearing. This property can be utilized in applications requiring strong and durable materials, such as textiles for sportswear, ropes, composites, or reinforcement fibers in construction materials.

4.6. Biodegradability

Feather fibers are biodegradable, as they are composed of natural proteins. Feathers rich in keratin can be utilized as a sustainable alternative to synthetic materials in various applications. These include packaging materials, biodegradable plastics, and biomedical scaffolds. This makes them an environmentally friendly option compared to synthetic fibers that persist in the environment for extended periods.

5. Conclusions

A comprehensive characterization of the physical and chemical properties of whole duck feathers from French mulard species, including their various categories and fractions (barbs, rachis, and calamus), was conducted. Through this analysis, chemical tests demonstrated the stability of feathers in aqueous media and nonpolar solvents, mild resistance to weak acids and bases, and poor resistance to strong acids and bases. Additionally, the feather's structural composition, consisting of mainly pure fiber keratin, was revealed. This included the regular arrangement of keratin fibers within the barbs, rachis, and calamus, as well as the honeycomb structure of the rachis. With their rich keratin content, heating properties, hydrophobic properties, honeycomb structure, and biodegradability, feathers offer the potential for producing valuable bioproducts such as cosmetics, fertilizers, activated carbon, waterproof materials, lightweight textiles, construction components, thermal insulation, and biodegradable alternatives. This opens up exciting opportunities for their multifaceted application in a wide range of industries and environmental initiatives.

References

1. Irshad, A.; Sharma, B.D. Abattoir by-Product Utilization for Sustainable Meat Industry: A Review. *J. Anim. Prod. Adv.* **2015**, *5*, 681. [CrossRef]
2. Lasekan, A.; Abu Bakar, F.; Hashim, D. Potential of chicken by-products as sources of useful biological resources. *Waste Manag.* **2013**, *33*, 552–565. [CrossRef] [PubMed]
3. Tesfaye, T.; Sithole, B.; Ramjugernath, D. Valorisation of chicken feathers: A review on recycling and recovery route—Current status and future prospects. *Clean Technol. Environ. Policy* **2017**, *19*, 2363–2378. [CrossRef]
4. Beylot, A.; Hochar, A.; Michel, P.; Descat, M.; Ménard, Y.; Villeneuve, J. Municipal Solid Waste Incineration in France: An Overview of Air Pollution Control Techniques, Emissions, and Energy Efficiency. *J. Ind. Ecol.* **2018**, *22*, 1016–1026. [CrossRef]
5. Agreste. *Filière Palmipèdes Gras*; Agreste: Limoges, France, 2017.
6. Rochlitz, I.; Broom, D.M. The welfare of ducks during foie gras production. *Anim. Welf.* **2017**, *26*, 135–149. [CrossRef]
7. Franke-Whittle, I.H.; Insam, H. Treatment alternatives of slaughterhouse wastes, and their effect on the inactivation of different pathogens: A review. *Crit. Rev. Microbiol.* **2013**, *39*, 139–151. [CrossRef]
8. Brandelli, A.; Sala, L.; Kalil, S.J. Microbial enzymes for bioconversion of poultry waste into added-value products. *Food Res. Int.* **2015**, *73*, 3–12. [CrossRef]
9. Kondamudi, N.; Strull, J.; Misra, M.; Mohapatra, S.K. A green process for producing biodiesel from feather meal. *J. Agric. Food Chem.* **2009**, *57*, 6163–6166. [CrossRef]
10. Campos, I.; Pinheiro Valente, L.M.; Matos, E.; Marques, P.; Freire, F. Life-cycle assessment of animal feed ingredients: Poultry fat, poultry by-product meal and hydrolyzed feather meal. *J. Clean. Prod.* **2020**, *252*, 119845. [CrossRef]
11. Saravanan, K.; Dhurai, B. Exploration on amino acid content and morphological structure in chicken feather fiber. *J. Text. Apparel, Technol. Manag.* **2012**, *7*, 1–6.
12. Bulaj, G. Formation of disulfide bonds in proteins and peptides. *Biotechnol. Adv.* **2005**, *23*, 87–92. [CrossRef]
13. Alibardi, L. Immunolocalization of alpha-keratins and feather beta-proteins in feather cells and comparison with the general process of cornification in the skin of mammals. *Ann. Anat.* **2013**, *195*, 189–198. [CrossRef]
14. Wang, B.; Yang, W.; McKittrick, J.; Meyers, M.A. Keratin: Structure, mechanical properties, occurrence in biological organisms, and efforts at bioinspiration. *Prog. Mater. Sci.* **2016**, *76*, 229–318. [CrossRef]
15. Chaitanya Reddy, C.; Khilji, I.A.; Gupta, A.; Bhuyar, P.; Mahmood, S.; Saeed AL-Japairai, K.A.; Chua, G.K. Valorization of keratin waste biomass and its potential applications. *J. Water Process Eng.* **2021**, *40*, 101707. [CrossRef]
16. Tesfaye, T.; Sithole, B.; Ramjugernath, D.; Chunilall, V. Valorisation of chicken feathers: Characterisation of chemical properties. *Waste Manag.* **2017**, *68*, 626–635. [CrossRef]
17. Zhan, M.; Wool, R.P. Mechanical properties of chicken feather fibers. *Polym. Compos.* **2011**, *32*, 937–944. [CrossRef]
18. Parikh, J.; Channiwala, S.A.; Ghosal, G.K. A correlation for calculating HHV from proximate analysis of solid fuels. *Fuel* **2005**, *84*, 487–494. [CrossRef]
19. Jiang, B.; Tsao, R.; Li, Y.; Miao, M. Food Safety: Food Analysis Technologies/Techniques. *Encycl. Agric. Food Syst.* **2014**, *3*, 273–288. [CrossRef]
20. Laemmli, U.K. Cleavage of structural proteins during the assembly of the head of bacteriophage T4. *Nature* **1970**, *227*, 680–685. [CrossRef]
21. Kluska, J.; Kardaś, D.; Heda, Ł.; Szumowski, M.; Szuszkiewicz, J. Thermal and chemical effects of turkey feathers pyrolysis. *Waste Manag.* **2016**, *49*, 411–419. [CrossRef] [PubMed]
22. Ingham, P.E. Pyrolysis of wool and the action of flame retardants. *J. Appl. Polym. Sci.* **1971**, *15*, 3025–3041. [CrossRef]

23. Ronsse, F.; van Hecke, S.; Dickinson, D.; Prins, W. Production and characterization of slow pyrolysis biochar: Influence of feedstock type and pyrolysis conditions. *GCB Bioenergy* **2013**, *5*, 104–115. [CrossRef]

24. Kwiatkowski, K.; Krzysztoforski, J.; Bajer, K.; Dudyński, M. Gasification of Feathers for Energy Production—A Case Study. In Proceedings of the 20th European Biomass Conference and Exhibition, Milan, Italy, 18–22 June 2012; pp. 1858–1862. [CrossRef]

25. Rohman, A.; Che Man, Y.B. FTIR spectroscopy combined with chemometrics for analysis of lard in the mixtures with body fats of lamb, cow, and chicken. *Int. Food Res. J.* **2010**, *17*, 519–526.

26. Poole, A.J.; Church, J.S.; Huson, M.G. Environmentally sustainable fibers from regenerated protein. *Biomacromolecules* **2009**, *10*, 1–8. [CrossRef] [PubMed]

27. Slangen, K.J. Patent Application Publication. U.S. Patent 2007/0260043 A1, 7 June 2007.

28. Lee, B.; Richards, F.M. The interpretation of protein structures: Estimation of static accessibility. *J. Mol. Biol.* **1971**, *55*, 379–400. [CrossRef]

29. Finney, J.L. Volume occupation, environment, and accessibility in proteins. Environment and molecular area of RNase-S. *J. Mol. Biol.* **1978**, *119*, 415–441. [CrossRef]

30. Shrake, A.; Rupley, J.A. Environment and exposure to solvent of protein atoms. Lysozyme and insulin. *J. Mol. Biol.* **1973**, *79*, 361–371. [CrossRef] [PubMed]

31. Magnusson, K.E. The hydrophobic effect and how it can be measured with relevance for cell–cell interactions. *Scand. J. Infect. Dis. Suppl.* **1980**, (Suppl. 24), 131–134.

32. Miwa, M.; Nakajima, A.; Fujishima, A.; Hashimoto, K.; Watanabe, T. Colloids Surf. *Org. Coat. Appl. Polym. Sci. Proc* **1999**, *15*.

33. Liu, Y.; Chen, X.; Xin, J.H. Hydrophobic duck feathers and their simulation on textile substrates for water repellent treatment. *Bioinspiration Biomim.* **2008**, *3*, 046007. [CrossRef]

34. Roach, P.; Shirtcliffe, N.J.; Newton, M.I. Progess in superhydrophobic surface development. *Soft Matter* **2008**, *4*, 224–240. [CrossRef]

35. Quéré, D.; Reyssat, M. Non-adhesive lotus and other hydrophobic materials. *Philos. Trans. R. Soc. A Math. Phys. Eng. Sci.* **2008**, *366*, 1539–1556. [CrossRef]

36. Nosonovsky, M.; Bhushan, B. Biologically inspired surfaces: Broadening the scope of roughness. *Adv. Funct. Mater.* **2008**, *18*, 843–855. [CrossRef]

37. Richards, F.M. Areas, volumes, packing, and protein structure. *Annu. Rev. Biophys. Bioeng.* **1977**, *6*, 151–176. [CrossRef] [PubMed]

38. Finney, J.L. The organization and function of water in protein crystals. *Philos. Trans. R. Soc. Lond. B. Biol. Sci.* **1977**, *278*, 3–32. [CrossRef]

39. Cozzone, A.J. Proteins: Fundamental Chemical Properties. *eLS* **2002**, 1–10. [CrossRef]

40. Sharma, S.; Gupta, A.; Saufi, S.M.; Kee, C.Y.G.; Podder, P.K.; Subramaniam, M.; Thuraisingam, J. Study of different treatment methods on chicken feather biomass. *IIUM Eng. J.* **2017**, *18*, 47–55. [CrossRef]

41. Pourjavaheri-Jad, F.; Shanks, R.; Czajka, M.; Gupta, A. Purification and Characterisation of Feathers prior to Keratin Extraction. In Proceedings of the 8th International Chemical Engineering Congress & Exhibition (IChEC 2014), Kish, Iran, 24–27 February 2014.

42. Kong, J.; Yu, S. Fourier transform infrared spectroscopic analysis of protein secondary structures. *Acta Biochim. Biophys. Sin.* **2007**, *39*, 549–559. [CrossRef] [PubMed]

43. Barth, A. Infrared spectroscopy of proteins. *Biochim. Biophys. Acta Bioenerg.* **2007**, *1767*, 1073–1101. [CrossRef] [PubMed]

44. Haris, P.I.; Severcan, F. FTIR spectroscopic characterization of protein structure in aqueous and non-aqueous media. *J. Mol. Catal. B Enzym.* **1999**, *7*, 207–221. [CrossRef]

45. Jackson, M.; Mantsch, H.H. The use and misuse of FTIR spectroscopy in the determination of protein structure. *Crit. Rev. Biochem. Mol. Biol.* **1995**, *30*, 95–120. [CrossRef]

46. Menefee, E.; Yee, G. Thermally-Induced Structural Changes in Wool. *Text. Res. J.* **1956**, *35*, 801–812. [CrossRef]

47. Spei, M.; Holzem, R. Thermoanalytical investigations of extended and annealed keratins. *Colloid Polym. Sci.* **1987**, *265*, 965–970. [CrossRef]

48. Alahyaribeik, S.; Ullah, A. Methods of keratin extraction from poultry feathers and their effects on antioxidant activity of extracted keratin. *Int. J. Biol. Macromol.* **2020**, *148*, 449–456. [CrossRef]

49. Khosa, M.A.; Wu, J.; Ullah, A. Chemical modification, characterization, and application of chicken feathers as novel biosorbents. *RSC Adv.* **2013**, *3*, 20800–20810. [CrossRef]

50. Sullivan, T.N.; Pissarenko, A.; Herrera, S.A.; Kisailus, D.; Lubarda, V.A.; Meyers, M.A. A lightweight, biological structure with tailored stiffness: The feather vane. *Acta Biomater.* **2016**, *41*, 27–39. [CrossRef] [PubMed]

51. Donato, R.K.; Mija, A. Keratin associations with synthetic, biosynthetic and natural polymers: An extensive review. *Polymers* **2020**, *12*, 32. [CrossRef] [PubMed]

52. Feroz, S.; Muhammad, N.; Ranayake, J.; Dias, G. Keratin—Based materials for biomedical applications. *Bioact. Mater.* **2020**, *5*, 496–509. [CrossRef]

53. Kovalev, A.; Filippov, A.E.; Gorb, S.N. Unzipping bird feathers. *J. R. Soc. Interface* **2014**, *11*, 20130988. [CrossRef]

54. Sullivan, T.N.; Wang, B.; Espinosa, H.D.; Meyers, M.A. Extreme lightweight structures: Avian feathers and bones. *Mater. Today* **2017**, *20*, 377–391. [CrossRef]

55. Idris, A.; Vijayaraghavan, R.; Patti, A.F.; Macfarlane, D.R. Distillable protic ionic liquids for keratin dissolution and recovery. *ACS Sustain. Chem. Eng.* **2014**, *2*, 1888–1894. [CrossRef]

56. Yoshimizu, H.; Mimura, H.; Ando, I. 13C CP /MAS NMR Study of the Conformation of Stretched or Heated Low-Sulfur Keratin Protein Films. *Macromolecules* **1991**, *24*, 862–866. [CrossRef]

57. Utiu, L.; Demco, D.E.; Fechete, R.; Möller, M.; Popescu, C. Morphology and molecular dynamics of hard α-keratin based micro-tubes by ^{1}H and ^{13}C solid-state NMR. *Chem. Phys. Lett.* **2011**, *517*, 86–91. [CrossRef]

58. Duer, M.J.; McDougal, N.; Murray, R.C. A solid-state NMR study of the structure and molecular mobility of α-keratin. *Phys. Chem. Chem. Phys.* **2003**, *5*, 2894–2899. [CrossRef]

59. Idris, A.; Vijayaraghavan, R.; Rana, U.A.; Fredericks, D.; Patti, A.F.; MacFarlane, D.R. Dissolution of feather keratin in ionic liquids. *Green Chem.* **2013**, *15*, 525–534. [CrossRef]